Energy efficiency and thermal environment of floor heating system using heat pump

S. Kindaichi, S. Kim, Y. Akamine,
M. Mae, and Y. Sakamoto
The University of Tokyo

ABSTRACT

This paper describes thermal characteristics of a hydronic floor heating system using heat pumps. An experimental system is constructed in a climate chamber. It has a test room with a floor area of 11.6 m^2 and an air volume of 23.15 m^3. Higher heat flow from floor heating can be seen in the room space at cases using panels with a thinner top layer made by materials with lower thermal resistance. Such panels also provide higher room temperature than other ones in comparison with conditions at similar supply water temperature.

The heat balance in the whole system is observed. The ratio of heat available for space heating is almost half of the input heat. Reduction of the heat loss is necessary to improve the system thermal efficiency.

1. INTRODUCTION

Generally in residential houses in Japan, the energy consumption for space cooling is only a few percent of the total consumption, while that for space heating accounts for the rather large ratio and reaches around 30% on average. Improvement of thermal insulation and air tightness of the building envelope has been led to reduction of the heat load, where hydronic heating systems with lower water temperatures are probably available.

In terms of the air conditioning system, heating systems using heat pumps may provide further energy saving. Coefficient of performance (COP) of heat pumps is changed significantly by operating conditions. Especially higher COP is obtained by decrease of supply water temperature. Therefore, the combination of hydronic floor heating and heat pumps may be a possible solution to obtain not only the adaptive thermal comfort but the sufficient energy efficiency under suitable operation.

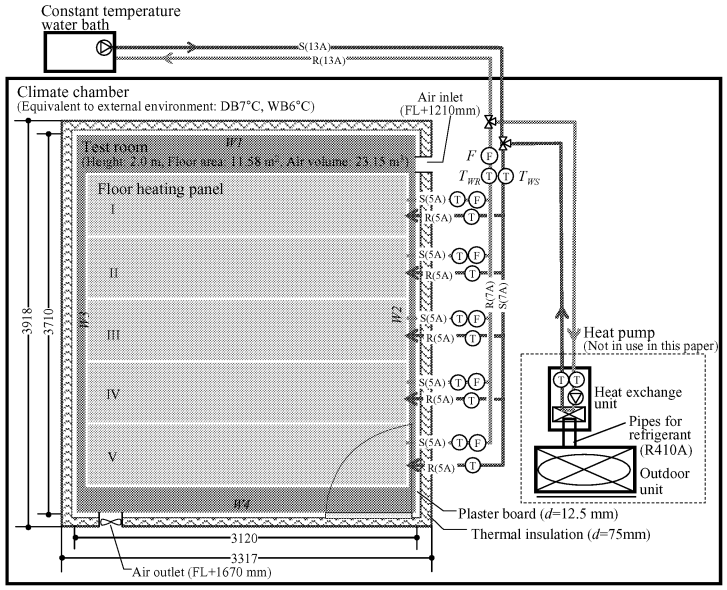

Ⓣ : T type (Cu-Co) thermocouple
Ⓕ : Magnetic flow meter
▽ : Circulation pump
S(*): Supply water piping
R(*): Return water piping
*: Nominal diameter (7A or 5A)

	Internal diameter [mm]	Wall thickness [mm]	Material
7A	6.8	1.6	Cross linked polyethylene pipe
5A	4.8	1.6	

Figure 1 System configuration of the experimental system

Table 1 Measuring items and measuring points

Section			Measuring item	Measuring point		Sensor / Equipment
Test room	Heating panel	Upper surface	Temperature	45		T type thermocouple
			Temperature distribution	1		Infrared thermal camera
			Heat flux	15	3 per each panel × 5 panels	Heat flow sensor*1
		Under surface	Temperature	12		T type thermocouple
			Heat flux	25	5 per each panel × 5 panels	Heat flow sensor*1
	Wall surface	Inner	Temperature	28	7 per each wall × 4 walls	T type thermocouple
			Heat flux	22		Heat flow sensor*1
		Outer	Temperature	28	7 per each wall × 4 walls	T type thermocouple
	Inner surface of ceiling		Temperature	9		T type thermocouple
			Heat flux	3		Heat flow sensor*1
	Room space		Air temperature	45	9 points × 5 heights (FL+100, 500, 750, 1100, 1900 mm)	T type thermocouple
			Humidity	1	Center point at FL+750 mm	Macromolecule humidity sensor
			Globe temperature	18	9 points × 2 heights (FL+100, +750 mm)	Globe thermometer (75 mmϕ) + T type thermocouple
			PMV	1	Center point at FL+750 mm	Portable measuring set
Outside (Climate chamber)			Air temperature	4	1 per near each wall × 4 walls	T type thermocouple
			Humidity	1	Near *WI*	Macromolecule humidity sensor
Heating medium (Water)			Temperature	12	Supply: T_{WS} [°C] Return: T_{WR} [°C] * Figure 1	T type thermocouple (Sheath type)
			Flow rate	6	*F* [*l*/min] * Figure 1	Magnetic flow meter

*1 Dimention [mm] ($l \times w \times t$): 310 × 310 × 0.7

2. EXPERIMENTAL SETUP

2.1 Experimental test room

An experimental system was constructed in a climate chamber, in which temperature and humidity can be kept constant. Figure 1 shows a system configuration. The test room has insulated external walls and a heat loss coefficient of 2.35 W/(m^2·K), which is better than the Japan's standard for residential buildings in the moderate climate region. The test room also has a floor area of 11.58 m^2 and an air volume of 23.15 m^3.

There are two kinds of heat sources: a constant temperature water bath and an air source heat pump unit, but only the experiments with former one are reported in this paper. Hot water generated in the heat source is supplied to the test room by floor heating through five parallel piping with 5A in nominal diameter.

2.2 Measuring items and measuring points

Table 1 shows measuring items and the points. Heat flux on the floor, walls and ceiling of the test room is measured by heat flow sensors with 310 mm square. Room temperatures are measured by T type thermocouples at 5 points in the vertical direction and 9 points in the horizontal one. Supply water temperature T_{WS} and return water temperature T_{WR} are measured in the water piping. Water flow rate F is measured by a magnetic flow meter. Each item is measured every 10 seconds.

2.3 Floor heating panels

Five kinds of floor heating panels shown in Table 2 were adopted in the experiment. Each panel is laid on plywood. Piping is buried in the top layer in the PanelA and in expanded polystyrene boards in the other panels. The PanelB has the thinnest top layer of 3.5 mm. The influences of intervals between pipes and the use of the alminum foils are compared among the three types of the PanelC.

2.4 Heat flow of the system

Figure 2 shows an image of heat flow of the system and expressions of each symbol. Heat input Q_{INPUT} is calculated by using supply and return water temperatures T_{WS} and T_{WR} and water flow rate F. Heat flows Q_{UP}, Q_{DOWN}, Q_{L_WALL} and Q_{L_CE} represent upward one from the floor surface in the test room, downward one from the floor heating panels, heat loss through the walls and heat loss from the ceiling respectively, and are obtained from the average measured ones. $\overline{T}_{0750}$ indicates an average room temperature, which is measured at FL+750mm high. Average floor temperature $\overline{T}_{floor}$ is also obtained from the 36 temperatures measured by the thermocouples.

Table 2 Description of floor heating panels

Panel	Section (*a*: Surface layer, *b*: Inner layer, *c*: Water pipe (5A), *d*: Aluminum foil)	Size of each panel [mm]	Heating area for 5 panels [m^2] (Heating ratio [%])	Thermal conductivity of surface layer λ [W/(m·K)]	Pipe pitch [mm]	Thickness of aluminum foil [mm]	Note
A	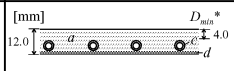	606×2718	8.24 (69.8)	0.124	75	0.05	Commercial Product
B	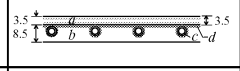	585×3000	8.78 (74.4)	0.205	75	0.08	Commercial product
C-75	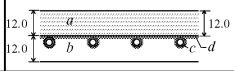	585×3000	8.78 (74.4)	0.117	75	0.08	Commercial product
C-50	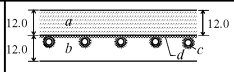	585×3000	8.78 (74.4)	0.117	50	0.08	Prototype
C-75(0)	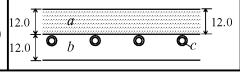	585×3000	8.78 (74.4)	0.117	75	-	Prototype

D_{min}*: Minimum distance between top of the pipe and floor surface

2.5 Experimental conditions

Experimental parameters are indicated in Table 3. Before each experiment, the whole system is cooled to the temperature in the external environment. In this paper, the constant temperature water bath is controlled so that the supply water temperature is kept at 30ºC for 24 hr as soon as one condition is started with a flow rate and a floor heating panel. After that, the set temperature is changed to 40ºC and 50ºC continuously for 24 hr each. Case2 is set as a basic condition, in which the water flow rate F follows the rated one listed in the catalog.

The followings are the results at steady state, which are extracted and averaged from the data at the last 3 hours in each condition.

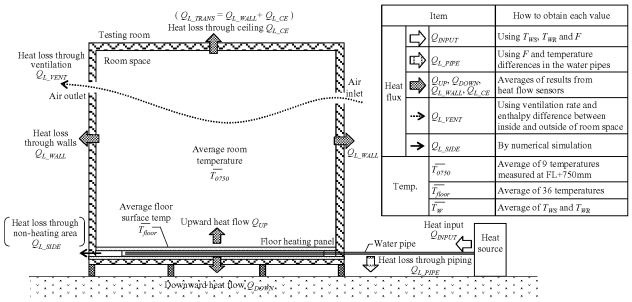

Figure 2 Heat flow of the system

Table 3 Experimental conditions

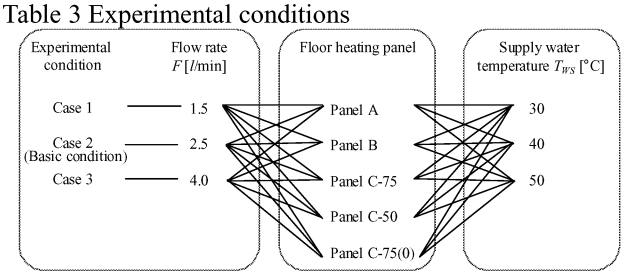

・Heat source: Constant temperature water bath
・Outside air: DB7°C, WB6°C ・Ventilation rate: 0.5 times/h
・Each condition is continued for 24 hours.

3. INDOOR THERMAL ENVIRONMENT

3.1 Heat supplied to the room space

Figure 3 compares the Q_{UP} and $\overline{T}_{0750}$ in each condition with a supply water temperature of 40ºC. The figure shows that the flow rate can be kept around the set value in every condition. Q_{UP} varies significantly between the kinds of the panel. $\overline{T}_{0750}$ can be kept higher as Q_{UP} becomes higher. The use of the PanelB provides the highest Q_{UP} in each case and higher $\overline{T}_{0750}$ of 26.6ºC in Case2 for example. On the other hand, Q_{UP} in PanelC-75(0) is decreased about 32% compared to that in the PanelC-75 which

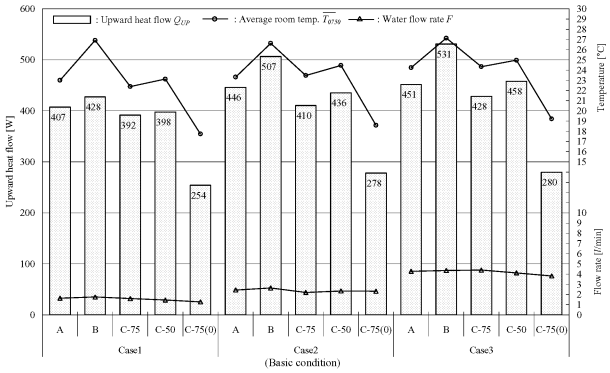

Figure 3 Upward heat flow and average room temperature in each panel (T_{WS}=40ºC)

has the same structure except for the aluminum foil. The use of a thin top layer with higher heat conductivity such as the PanelB may lead to decrease the supply water temperature and then efficient operation of heat pumps due to the high performance of thermal characteristics of the panel.

In Case2, Q_{UP} increases about 18% with an increase of the flow rate of 1.44 times compared to Case1 in the use of the PanelB. Similarly, the flow rate in Case3 becomes about 1.65 times as large as that in Case2. But the increase of Q_{UP} is seen only 4.7% in Case3 and is smaller relatively than the former comparison. This indicates that the setting of the rated flow rate, which is 0.5 *l*/min per one floor panel, is reasonable to show the adequate performance.

In actual use, upward heat flow is changed depending on the characteristics of panels, water temperature, water flow rate, room temperature and so on. Here, assuming that the upward heat flow depends on the temperature differences between water in the piping and room air, relationships in Figure 4 are obtained for each panel. From the figure, different values of $(\overline{T}_w - \overline{T}_{0750})$ are needed in each panel in order to obtain the same upward heat flow. For example, it is found that the use of PanelC-75(0) needs higher water temperature than the other panels if the room temperature $\overline{T}_{0750}$ is assumed to be the same.

3.2 Floor temperature distribution

Figure 5 shows floor temperature distributions in each panel taken by an infrared camera. The average temperature $\overline{T}_{floor}$ and the other ones just above the water piping and between the pipes measured by the thermocouples are also indicated in Table4.

Different ranges of the floor temperatures can be observed in each panel. The temperature distributions also vary depending on the position whether or not above the piping. In the panels of C-75 and C-50, the distributions are rather smaller than the PanelA and PanelB due to the thermal resistance in the thicker top layer. Compared PanelB to PanelA, the temperature difference between above the piping and not above the one is 1.0 K and much smaller than that in PanelA even though the top layer has a higher heat conductivity in the PanelB. This is

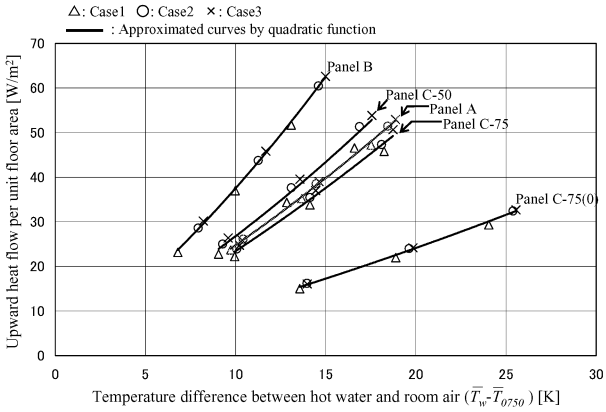

Figure 4 Relationships between temperature differences $(\overline{T}_w - \overline{T}_{0750})$ and upward heat flow in each panel

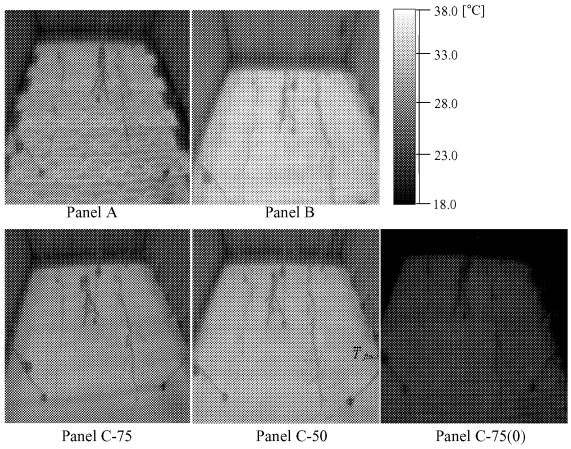

Figure 5 Floor temperature distributions taken by an infrared camera in each panel
(Case2, T_{WS}=40ºC)

Table 4 Floor temperatures measured by thermocouples

Panel	Average floor temperature [ºC]			Temperature difference [K]
	$\overline{T}_{floor}$ [ºC]	just above the pipes [ºC]	between the pipes [ºC]	
A	28.5	29.6	27.1	2.5
B	31.7	32.4	31.4	1.0
C-75	27.9	28.2	27.6	0.6
C-50	29.0	29.2	28.8	0.4
C-75(0)	22.0	22.8	21.4	1.4

probably due to the position of the aluminum foil. In the PanelA, the aluminum layer is located downside of the piping, whereas the aluminum is around the piping and at the upper side of it in the PanelB. The structure may cause thermal diffusion in the horizontal direction before the top layer and ease the temperature distribution on the floor surface.

Therefore, the use of an aluminum foil over the piping is effective to obtain a relatively uniform floor temperature as well as higher upward heat

in the room space.

3.3 Room temperature distribution

Figure 6 shows vertical temperature distributions in the room space in each panel. The average ones in the heating area and non-heating area are shown. The figure also indicates a result conducted by an air conditioner (AC) in the same room. The indoor unit is installed on the top of the wall of W1.

Every case of floor heating shows uniform temperature distribution, in which the vertical differences of air temperatures are within 0.6ºC. Also, there are few temperature differences between at the heating area and non-heating one in these conditions with heating ratios of 70% and 74%.

Furthermore, significant differences of the temperature distribution can be seen between the cases of floor heating and that of AC. Compared the case of PanelC-50 to that of AC, which has a similar temperature at FL+0750mm, the vertical temperature difference reaches 5.8ºC at the AC case and only 0.5ºC at the case with PanelC-50.

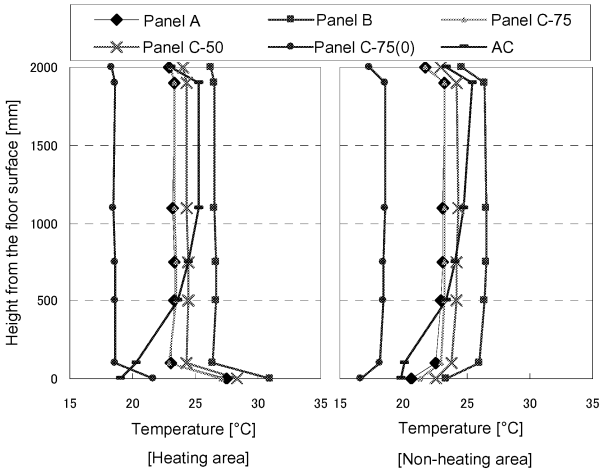

Figure 6 Vertical temperature distributions at floor heating and AC
(Floor heating: Case2, T_{WS}=40ºC)

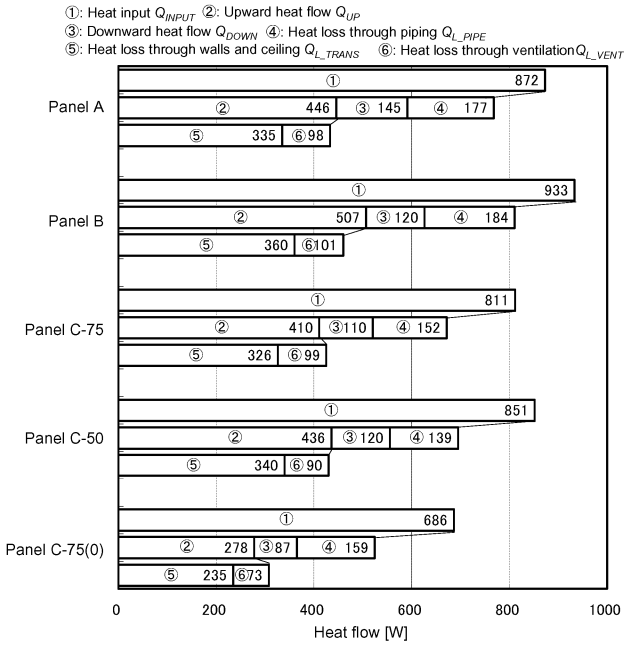

Figure 7 Heat input and heat losses obtained from the experiments (Case2, T_{WS}=40ºC)

4. HEAT BALANCE OF THE SYSTEM

4.1 Heat input and each heat loss

As shown in Figure 2, the part of the heat input changes into heat loss through the piping and to the under floor. Then the rest can be supplied to the room space. The supplied heat should be balanced with the heat loss through the walls and ceiling or ventilation at steady state.

Figure 7 shows each heat flow obtained from the experiments. In comparison between the input and output heat flows in the room space, the sum of Q_{L_TRANS} and Q_{L_VENT} is comparable to Q_{UP} and each difference is 5 to 10% in every case. On the other hand, in the whole system, the sums of Q_{UP}, Q_{DOWN} and Q_{L_PIPE} show 15 to 25% smaller than Q_{INPUT}. The differences seem to be due to accuracies of the sensors and measuring equipments, the errors during the calculation of each heat, the influence of heat loss which cannot be measured and so on.

4.2 Heat loss through the non-heating area

Here, further heat loss is discussed by numerical analysis (Yamauchi Planning Inc.). Figure 8 is a conceptual diagram of the calculation model. The target is a two-dimensional area including the edge of the piping and the non-heating area. The size of the mesh is 1 mm square at the piping and about 10 mm square at the other components on average. The boundary conditions are also shown in the figure. The overall heat transfer coefficients between indoor and outdoor are calculated from the expression (Kilkis, 1995) by using the measured temperatures.

As a result, heat loss through the non-heating area Q_{L_SIDE} can be calculated by multiplying the sum of the heat outflow through the 4 sides of the rectangle in the figure by the total boundary length in the experiment.

4.3 HEAT BALANCE OF THE SYSTEM

Finally the heat balance of the system is examined. Figure 9 shows Q_{UP}, Q_{DOWN} and Q_{L_PIPE} obtained by the measurement and Q_{L_SIDE} calculated in the previous section for each panel. "Others" means the differences of the sum of them from the heat input Q_{INPUT}. The figure also indicates the ratios of each element.
It is found that the total heat outflow can be balanced with the heat input at the rates of 92-93% in the cases with the PanelA and PanelB. On the other hand, the ratios of "others" account for 16-23% in the three cases with PanelC. The difference is probably due to accumulation of heat losses through air space between the top and the inner layers which is difficult to be measured in those three conditions.

The thermal efficiency of the system is expressed by the ratio of Q_{UP} to Q_{INPUT}. The highest efficiency can be seen at a case with the PanelB, whereas the value is about 54 %. The ratio of heat available for space heating is no more than the half of the input heat in these conditions. The rest mainly consists of the heat losses. Especially, the heat losses through the piping and that to the under floor reach around 20% and 15% respectively. Therefore, increase of the insulation is needed to improve the energy efficiency of the whole system in addition to the use of a panel with high thermal characteristics such as the PanelB.

5. CONCLUSIONS

The following summarizes the results reported in this paper.

1) The largest upward heat flow and highest room temperature can be observed in the use of the PanelB, in which the thickness of the top layer is 3.5 mm.
2) The temperature distribution on the floor surface is depended on the structure of the panel, especially the position of the alminum foil.

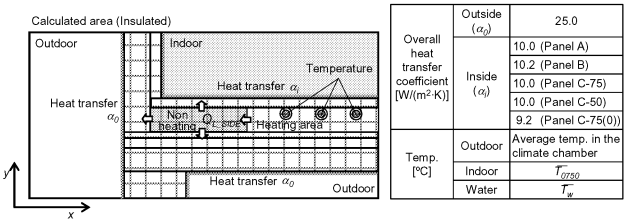

Figure 8 Conceptual diagram of the calculation model and the boundary conditions

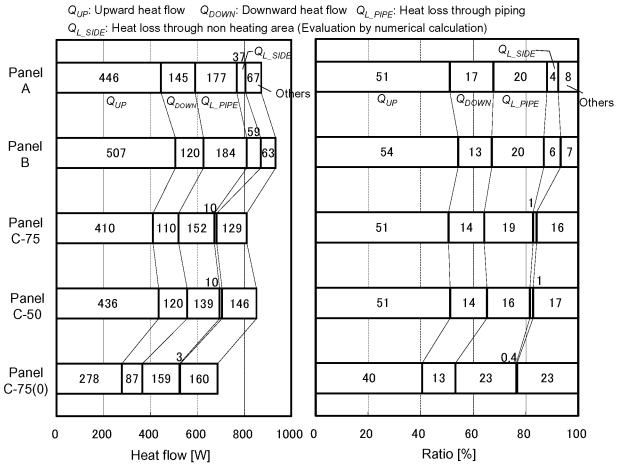

Figure 9 Heat balance of the system in each panel (Case2, T_{WS}=40ºC)

3) The heat balance of the system is analyzed by measurement and calculation. The ratio of heat available for space heating is about 50% of the heat input. Reduction of the heat loss in the piping or to the under floor is the most important issue to improve the energy efficiency in the whole system.

ACKNOWLEDGEMENTS

This work is supported by Ministry of Land, Infrastructure, Transport and Tourism of Japan.

REFERENCES

Kilkis, I. B. et al. (1995). A Simplified Model of Radiant In-Slab Heating Panels. ASHRAE Trans Vol.101 Part1: pp.210-216.

Yamauchi Planning Inc (2008.7.7). INSYS Ver.2.1.8. http://www.yp-i.co.jp/download/index.php